Acta Cryst E CRYSTALLOGRAPHIC COMMUNICATIONS

ISSN 2056-9890

Synthesis, crystal structure and Hirshfeld surface analysis of di-μ_2-chlorido-bis[(nitrato-κO)-bis(pyridine-κN)copper(II)]

Khadicha Toshboltaeva,[a] Khayit Khudaynazarovich Turaev,[a] Abdurasul Toshtemirov[a]* and Xolbek Zokirov[b]

[a]Termez State University, Barkamol avlod str. 43, Termez, 190100, Uzbekistan, and [b]University of Business and Science, Dostlik str. 14, Namangan, 160108, Uzbekistan. *Correspondence e-mail: tosabdurasul20@gmail.com

Received 20 July 2026
Accepted 16 October 2026

Edited by M. Weil, Vienna University of Technology, Austria

Keywords: crystal; copper; pyridine; synthesis; Hirshfeld surface analysis; hydrogen bonding.

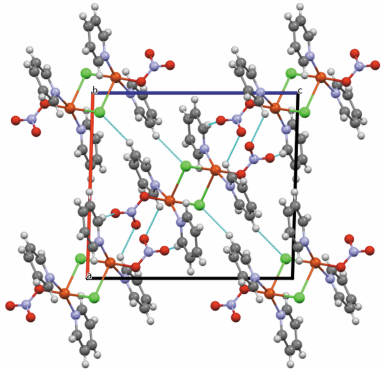
CCDC reference: 2494595

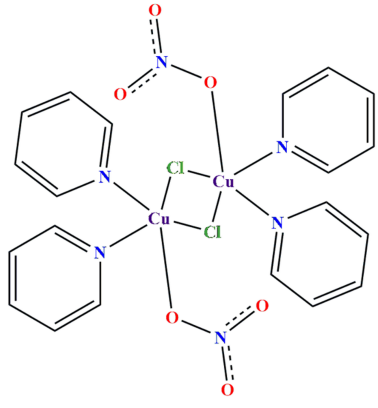
Supporting information: this article has supporting information at journals.iucr.org/e

The title compound, $[Cu_2Cl_2(NO_3)_2(C_5H_5N)_4]$, crystallizes as a centrosymmetric binuclear Cu^{II} complex in which the two central Cu^{II} atoms are interconnected by a pair of μ_2-chlorido bridges. The Cu^{II} atom is additionally coordinated by two pyridine N atoms and one O atom from a monodentate nitrato ligand, resulting in a distorted square-pyramidal coordination environment. In the crystal, the binuclear complexes are linked by C—H···Cl and C—H···O hydrogen bonds, generating a supramolecular framework structure. Hirshfeld surface analysis was performed to quantify and further elucidate the intermolecular interactions.

1. Chemical context

Copper(II) complexes continue to attract considerable interest in coordination chemistry owing to the structural diversity of the Cu^{II} coordination environments and the ability of ancillary ligands to generate mono- and multinuclear structures. Pyridine is a simple neutral N-donor ligand that readily coordinates to Cu^{II} and has been widely employed in the preparation of many different copper(II) complexes (Pandey, 2018; Bowmaker *et al.*, 2011). In copper(II) halide–pyridine systems, the nature of the halido ligand(s) and the coordination environment can lead to distinct molecular and extended structural motifs, in particular the ability of chlorido ligands to link symmetry-related copper(II) atoms through μ_2-binding modes into binuclear units (Bowmaker *et al.*, 2011; Herringer *et al.*, 2011).





In this context, the present work describes the synthesis and single-crystal X-ray characterization of a centrosymmetric

OPEN ACCESS
Published under a CC BY 4.0 licence

binuclear Cu^{II} complex, $[Cu_2(\mu_2\text{-}Cl)_2(\kappa O\text{-}NO_2)_2(C_5H_5N)_4]$, (**1**), together with an analysis of its intermolecular interactions.

2. Structural commentary

Compound (**1**) represents a centrosymmetric binuclear Cu^{II} molecular complex in which two copper(II) ions are connected by two μ_2-chlorido bridges, forming a $\{Cu_2Cl_2\}$ core. The Cu^{II} atom is five-coordinate, with two ligating pyridine nitrogen atoms (N1 and N2), one oxygen atom (O1) from a monodentate nitrate ligand, and the two bridging chloride ions (Fig. 1). The coordination environment of the Cu^{II} atom is distorted square-pyramidal, with the symmetry-related chlorido ligand Cl1($-x+1, -y+1, -z+1$) occupying the apical position. The five-coordinate geometry was assessed using the τ_5 parameter (Addison *et al.*, 1984). The calculated value of $\tau_5 = 0.18$ indicates a shape closer to square-pyramidal than trigonal-bipyramidal, consistent with the observed structural parameters.

The observed distortion around Cu^{II} in compound (**1**) may be discussed in the context of the Jahn–Teller effect characteristic of many Cu^{II} complexes (Hakimov *et al.*, 2025). The Cu—N bond lengths are 1.998 (3) and 2.000 (3) Å, while the Cu—O1 and basal Cu—Cl1 distances are 2.021 (2) and 2.3009 (10) Å, respectively. The apical Cu1—Cl1($-x+1, -y+1, -z+1$) bond is significantly longer at 2.7025 (10) Å, and the intradimer Cu···Cu separation is 3.4958 (7) Å. The angles in the basal plane, N—Cu—N = 167.24 (13)° and O—Cu—Cl = 177.77 (8)°, deviate from ideal values.

3. Supramolecular features

The crystal packing is consolidated by weak intermolecular C—H···O and C—H···Cl contacts, the numerical parameters of which are summarized in Table 1. The C—H···O interactions connect neighbouring molecules into layers parallel to (101). These layers are further linked by C—H···Cl contacts, resulting in a supramolecular framework structure (Fig. 2). In addition, π–π contacts between pyridine rings within the centrosymmetric dimer are present, with centroid-to-centroid distances of 4.201 (2) Å between *Cg*3 (ring N1/C1–C5) and *Cg*4($-x+1, -y+1, -z+1$) (ring N2/C6–C10), and a slippage of 1.457 Å.

Table 1
Hydrogen-bond geometry (Å, °).

D—H···A	D—H	H···A	D···A	D—H···A
C4—H4···O1^{i}	0.93	2.49	3.390 (5)	163
C5—H5···O2^{ii}	0.93	2.57	3.237 (4)	129
C2—H2···Cl1^{iii}	0.93	2.84	3.639 (4)	135

4. Hirshfeld surface analysis

A Hirshfeld surface analysis was performed using *CrystalExplorer* (Spackman *et al.*, 2021) to quantify the intermolecular contacts in the crystal structure. The Hirshfeld surface mapped over d_{norm} is shown in Fig. 3. The red regions on the surface indicate close intermolecular contacts, particularly C—H···O and C—H···Cl interactions, which contribute to the cohesion of the crystal packing. The two-dimensional fingerprint plots provide further insight into the relative contributions of the intermolecular contacts (Fig. 4). H···H contacts show the largest contribution to the Hirshfeld surface. The prominent H···O/O···H contacts are associated with C—H···O interactions and are characterized by sharp features in the corresponding fingerprint plot (McKinnon *et*

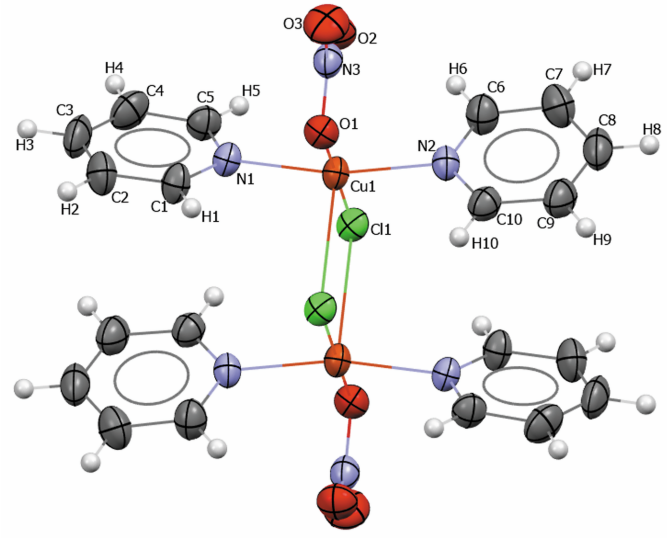


Figure 1
View of the title complex with the atom-numbering scheme of the asymmetric unit. Displacement ellipsoids are drawn at the 50% probability level; unlabelled atoms are related to the labelled atoms by symmetry operation $-x+1, -y+1, -z+1$.

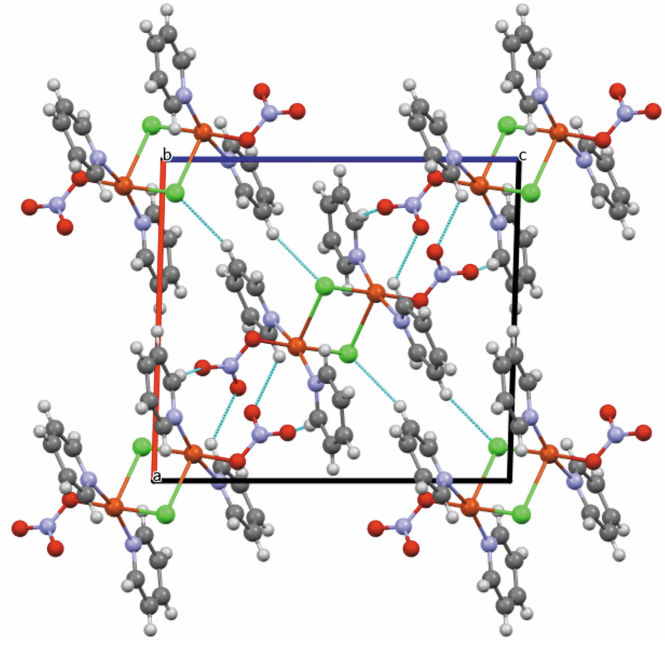


Figure 2
Packing plot of (**1**) in a view along [010]. C—H···O and C—H···Cl interactions are shown as turquoise dotted lines.

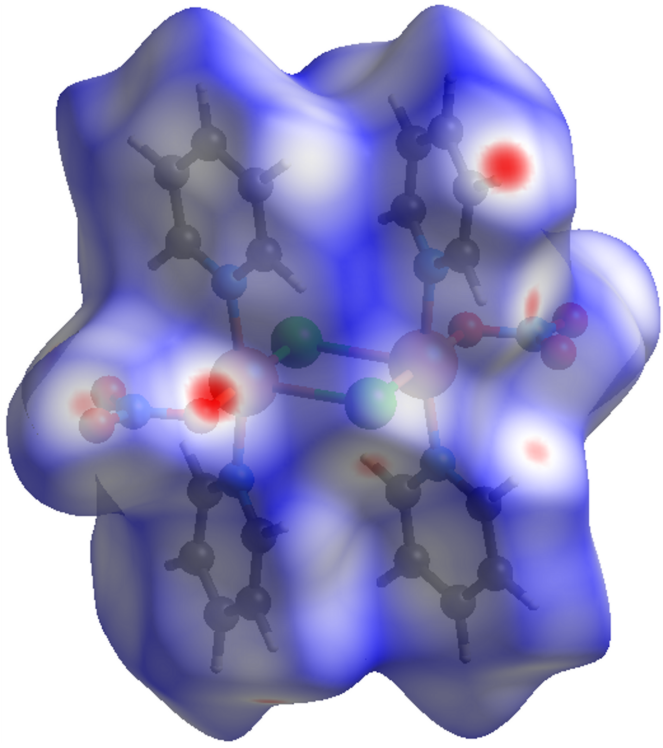


Figure 3
View of the three-dimensional Hirshfeld surface of the title compound plotted over d_{norm}.

al., 2007), consistent with directional close contacts. Similarly, the characteristic features in the H···Cl/Cl···H plot reflect intermolecular C—H···Cl contacts. The H···C/C···H and O···C/C···O contributions arise from additional close contacts involving the aromatic rings and oxygen atoms. Although these contacts are less prominent in the fingerprint analysis, they provide further insight into the intermolecular environment and the packing arrangement.

5. Database survey

A search of the Cambridge Structural Database (CSD, Version 2025.3.1; Groom *et al.*, 2016) for the di-μ_2-chlorido-bis[bis(pyridine-κN)(nitrato-κO)copper(II)] complex unit resulted in three hits, CSD refcodes COLZOT (Han *et al.*, 2008), VAVXUM (Atria *et al.*, 2004) and ZATQOA (Alvarez-Larena *et al.*, 1995). These structures and that of compound (**1**) comprise two central Cu^{II} atoms linked through two μ_2-chlorido ligands, forming a characteristic $\{Cu_2Cl_2\}$ core, while each copper(II) atom is in a five-coordinate environment involving oxygen and nitrogen donor atoms from the nitrate unit and different pyridine derivatives, respectively. Although COLZOT shares the Cu_2Cl_2 core with the title compound, its coordination environment differs significantly. In COLZOT, each Cu^{II} center is six-coordinate, with two pyridine nitrogen donors, two bridging chloride ions, one oxygen donor from a coordinated water molecule, and one oxygen donor from a nitrate ligand. This results in a distorted octahedral geometry, whereas the title compound contains five-coordinate Cu^{II} centers with a distorted square-pyramidal geometry. The key difference is the additional coordinated water molecule in COLZOT.

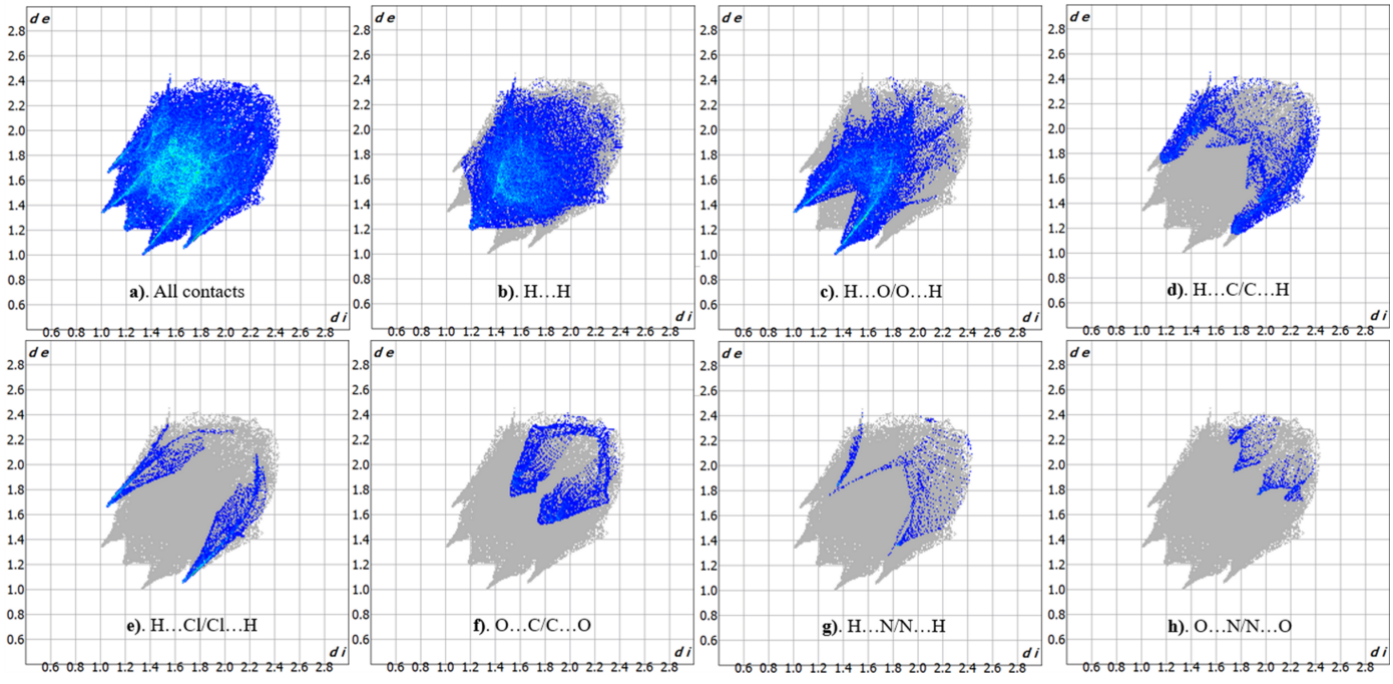


Figure 4
Two-dimensional fingerprint plots of (**1**) showing (*a*) all interactions, and delineated into (*b*) H···H (42.3%), (*c*) H···O/O···H (29.9%), (*d*) H···C/C···H (10.4%), (*e*) H···Cl/Cl···H (6.3%), (*f*) O···C/C···O (5.2%), (*g*) H···N/N···H (1.4%)and (*h*) O···N/N···O (1.4%) interactions.

6. Synthesis and crystallization

Pyridine (2 mmol, 158 mg) and $CuCl_2{\cdot}2H_2O$ (1 mmol, 170 mg) were placed in a glass vial, followed by the addition of distilled water (4 ml) and concentrated HNO_3 (1 ml). The mixture was stirred at room temperature for several minutes until a clear dark-blue solution was obtained. The solution was transferred to a 25 ml Teflon-lined stainless-steel autoclave, heated at 398 K for 48 h, and then cooled to 298 K at a rate of 10 K h^{-1} (Liu *et al.*, 2018). The resulting solution was transferred into a glass vial and kept in the dark at room temperature for four weeks, during which dark-blue prism-shaped crystals of $[Cu_2Cl_2(C_5H_5N)_4(NO_3)_2]$ formed. The crystals were isolated by filtration and dried at room temperature; yield 204 mg (64%, based on Cu), melting point 491–499 K.

7. Refinement

Crystal data, data collection and structure refinement details are summarized in Table 2. H atoms attached to C were positioned geometrically and refined using a riding model with distance constraints of C—H = 0.93 Å and with $U_{iso}(H) = 1.2U_{eq}(C)$.

Table 2
Experimental details.

Crystal data	
Chemical formula	$[Cu_2Cl_2(NO_3)_2(C_5H_5N)_4]$
M_r	638.40
Crystal system, space group	Monoclinic, $P2_1/n$
Temperature (K)	295
a, b, c (Å)	11.7560 (5), 8.1793 (3), 13.0074 (6)
β (°)	91.698 (4)
V (Å^3)	1250.19 (9)
Z	2
Radiation type	Cu $K\alpha$
μ (mm^{-1})	4.49
Crystal size (mm)	0.21 × 0.20 × 0.18
Data collection	
Diffractometer	Xcalibur, Ruby
Absorption correction	Multi-scan (*CrysAlis PRO*; Rigaku OD, 2020)
T_{min}, T_{max}	0.619, 1.000
No. of measured, independent and observed [$I > 2\sigma(I)$] reflections	3303, 1928, 1578
R_{int}	0.026
θ_{max} (°)	62.0
$(\sin\theta/\lambda)_{max}$ (Å^{-1})	0.573
Refinement	
$R[F^2 > 2\sigma(F^2)]$, $wR(F^2)$, S	0.039, 0.103, 1.04
No. of reflections	1928
No. of parameters	164
H-atom treatment	H-atom parameters constrained
$\Delta\rho_{max}$, $\Delta\rho_{min}$ (e Å^{-3})	0.50, −0.34

Computer programs: *CrysAlis PRO* (Rigaku OD, 2020), *SHELXT* (Sheldrick, 2015*a*), *SHELXL* (Sheldrick, 2015*b*), *OLEX2* (Dolomanov *et al.*, 2009) and *publCIF* (Westrip, 2010).

Acknowledgements

The authors thank the Institute of Bioorganic Chemistry of the Academy of Sciences of Uzbekistan, Tashkent, Uzbekistan for providing the single-crystal XRD facility.

References

Addison, A. W., Rao, T. N., Reedijk, J., van Rijn, J. & Verschoor, G. C. (1984). *J. Chem. Soc. Dalton Trans.* pp. 1349–1356.

Alvarez-Larena, A., Briansó-Penalva, J. L., Piniella, J. F., Moreno-Esparza, R., Ruiz-Ramírez, L. & Tovar, A. (1995). *Z. Kristallogr.* **210**, 543–544.

Atria, A. M., Cortés, P., Acevedo, L., Trujillo, R., Manzur, J., Peña, O. & Baggio, R. (2004). *J. Chil. Chem. Soc.* **49**, 341–344.

Bowmaker, G. A., Di Nicola, C., Pettinari, C., Skelton, B. W., Somers, N. & White, A. H. (2011). *Dalton Trans.* **40**, 5102–5115.

Dolomanov, O. V., Bourhis, L. J., Gildea, R. J., Howard, J. A. K. & Puschmann, H. (2009). *J. Appl. Cryst.* **42**, 339–341.

Groom, C. R., Bruno, I. J., Lightfoot, M. P. & Ward, S. C. (2016). *Acta Cryst.* B**72**, 171–179.

Hakimov, M., Ortikov, I., Sattarov, T., Tashkhodjaev, B. & Tojiboev, A. (2025). *Acta Cryst.* E**81**, 271–274.

Han, K.-F., Wu, H.-Y., Wang, Z.-M. & Guo, H.-Y. (2008). *Acta Cryst.* E**64**, m1607–m1608.

Herringer, S. N., Turnbull, M. M., Landee, C. P. & Wikaira, J. L. (2011). *Dalton Trans.* **40**, 4242–4252.

Liu, T., Wang, Y.-A., Zang, Q. & Zhong, G.-Q. (2018). *Bioinorg. Chem. Appl.* 8459638.

McKinnon, J. J., Jayatilaka, D. & Spackman, M. A. (2007). *Chem. Commun.* pp. 3814–3816.

Pandey, P. P. (2018). Pyridine. London: IntechOpen.

Rigaku OD (2020). *CrysAlis PRO*. Rigaku Oxford Diffraction, Yarnton, England.

Sheldrick, G. M. (2015*a*). *Acta Cryst.* A**71**, 3–8.

Sheldrick, G. M. (2015*b*). *Acta Cryst.* C**71**, 3–8.

Spackman, P. R., Turner, M. J., McKinnon, J. J., Wolff, S. K., Grimwood, D. J., Jayatilaka, D. & Spackman, M. A. (2021). *J. Appl. Cryst.* **54**, 1006–1011.

Westrip, S. P. (2010). *J. Appl. Cryst.* **43**, 920–925.

supporting information

Acta Cryst. (2026). E**82**, 1358-1361 [https://doi.org/10.1107/S2056989026010728]

Synthesis, crystal structure and Hirshfeld surface analysis of di-μ_2-chlorido-bis-[(nitrato-κO)bis(pyridine-κN)copper(II)]

Khadicha Toshboltaeva, Khayit Khudaynazarovich Turaev, Abdurasul Toshtemirov and Xolbek Zokirov

Computing details

Di-μ_2-chlorido-bis[(nitrato-κO)bis(pyridine-κN)copper(II)]

Crystal data

$[Cu_2Cl_2(NO_3)_2(C_5H_5N)_4]$
M_r = 638.40
Monoclinic, $P2_1/n$
a = 11.7560 (5) Å
b = 8.1793 (3) Å
c = 13.0074 (6) Å
β = 91.698 (4)°
V = 1250.19 (9) Å^3
Z = 2
$F(000)$ = 644
D_x = 1.696 Mg m^{-3}
Cu $K\alpha$ radiation, λ = 1.54184 Å
Cell parameters from 1423 reflections
θ = 6.6–62.2°
μ = 4.49 mm^{-1}
T = 295 K
Block, clear blue
0.21 × 0.20 × 0.18 mm

Data collection

Xcalibur, Ruby diffractometer
Detector resolution: 10.2576 pixels mm^{-1}
ω scans
Absorption correction: multi-scan (CrysAlisPro; Rigaku OD, 2020)
T_{min} = 0.619, T_{max} = 1.000
3303 measured reflections
1928 independent reflections
1578 reflections with $I > 2\sigma(I)$
R_{int} = 0.026
θ_{max} = 62.0°, θ_{min} = 5.0°
h = −10→13
k = −8→9
l = −14→12

Refinement

Refinement on F^2
Least-squares matrix: full
$R[F^2 > 2\sigma(F^2)]$ = 0.039
$wR(F^2)$ = 0.103
S = 1.04
1928 reflections
164 parameters
0 restraints
Primary atom site location: iterative
Hydrogen site location: inferred from neighbouring sites
H-atom parameters constrained
$w = 1/[\sigma^2(F_o^2) + (0.0515P)^2]$ where $P = (F_o^2 + 2F_c^2)/3$
$(\Delta/\sigma)_{max}$ = 0.001
$\Delta\rho_{max}$ = 0.50 e Å^{-3}
$\Delta\rho_{min}$ = −0.34 e Å^{-3}
Extinction correction: SHELXL2019/2 (Sheldrick, 2015b), $Fc^*=kFc[1+0.001xFc^2\lambda^3/\sin(2\theta)]^{-1/4}$
Extinction coefficient: 0.0040 (3)

Special details

Geometry. All esds (except the esd in the dihedral angle between two l.s. planes) are estimated using the full covariance matrix. The cell esds are taken into account individually in the estimation of esds in distances, angles and torsion angles; correlations between esds in cell parameters are only used when they are defined by crystal symmetry. An approximate (isotropic) treatment of cell esds is used for estimating esds involving l.s. planes.

Fractional atomic coordinates and isotropic or equivalent isotropic displacement parameters (Å²)

	x	*y*	*z*	U_{iso}*/U_{eq}
Cu1	0.41702 (4)	0.50764 (6)	0.60920 (4)	0.0344 (2)
Cl1	0.39492 (7)	0.34861 (10)	0.46408 (6)	0.0378 (3)
O1	0.4407 (2)	0.6529 (3)	0.73372 (19)	0.0417 (6)
O2	0.2887 (2)	0.5160 (3)	0.7709 (2)	0.0531 (8)
N1	0.5022 (2)	0.3299 (3)	0.6834 (2)	0.0362 (7)
N2	0.3024 (3)	0.6668 (3)	0.5523 (2)	0.0373 (7)
O3	0.3510 (3)	0.7100 (4)	0.8724 (2)	0.0644 (9)
N3	0.3575 (3)	0.6260 (4)	0.7945 (2)	0.0426 (8)
C1	0.6025 (3)	0.3566 (5)	0.7304 (3)	0.0441 (10)
H1	0.633957	0.460729	0.727360	0.053*
C10	0.3302 (4)	0.8169 (5)	0.5222 (3)	0.0445 (10)
H10	0.405587	0.850344	0.529814	0.053*
C5	0.4567 (3)	0.1802 (5)	0.6898 (3)	0.0450 (10)
H5	0.386417	0.160124	0.657634	0.054*
C6	0.1935 (4)	0.6214 (5)	0.5431 (3)	0.0519 (11)
H6	0.172908	0.517588	0.564971	0.062*
C9	0.2519 (4)	0.9237 (5)	0.4803 (3)	0.0559 (12)
H9	0.274166	1.027395	0.459501	0.067*
C4	0.5108 (4)	0.0548 (5)	0.7428 (4)	0.0591 (12)
H4	0.477106	−0.047810	0.746832	0.071*
C3	0.6148 (4)	0.0839 (5)	0.7891 (3)	0.0599 (13)
H3	0.653637	0.000928	0.824276	0.072*
C8	0.1408 (4)	0.8762 (6)	0.4695 (3)	0.0581 (12)
H8	0.086473	0.946167	0.440424	0.070*
C2	0.6609 (4)	0.2379 (6)	0.7828 (3)	0.0571 (12)
H2	0.731328	0.260742	0.814085	0.069*
C7	0.1111 (4)	0.7233 (6)	0.5025 (3)	0.0591 (12)
H7	0.035716	0.688927	0.497299	0.071*

Atomic displacement parameters (Å²)

	U^{11}	U^{22}	U^{33}	U^{12}	U^{13}	U^{23}
Cu1	0.0372 (4)	0.0333 (3)	0.0324 (4)	0.0025 (2)	−0.0061 (2)	0.0012 (2)
Cl1	0.0398 (5)	0.0382 (5)	0.0350 (5)	−0.0069 (4)	−0.0046 (4)	−0.0019 (4)
O1	0.0409 (15)	0.0408 (14)	0.0435 (15)	−0.0016 (12)	0.0011 (12)	−0.0033 (12)
O2	0.0487 (18)	0.0548 (17)	0.0559 (19)	−0.0097 (15)	0.0026 (14)	−0.0025 (14)
N1	0.0401 (18)	0.0338 (17)	0.0344 (17)	0.0018 (14)	−0.0053 (13)	0.0036 (13)
N2	0.0387 (18)	0.0362 (17)	0.0365 (17)	0.0071 (14)	−0.0064 (13)	0.0002 (14)
O3	0.085 (2)	0.0627 (19)	0.0459 (18)	0.0058 (17)	0.0107 (16)	−0.0184 (16)

N3	0.047 (2)	0.0409 (18)	0.0398 (19)	0.0111 (17)	−0.0020 (16)	0.0024 (16)
C1	0.049 (2)	0.038 (2)	0.045 (2)	−0.0009 (19)	−0.0158 (19)	0.0025 (18)
C10	0.051 (2)	0.038 (2)	0.045 (2)	0.0025 (19)	0.0019 (19)	0.0039 (19)
C5	0.043 (2)	0.042 (2)	0.051 (2)	−0.0078 (19)	−0.0021 (18)	0.0065 (19)
C6	0.051 (3)	0.044 (2)	0.061 (3)	0.002 (2)	−0.008 (2)	0.006 (2)
C9	0.068 (3)	0.042 (2)	0.058 (3)	0.014 (2)	0.006 (2)	0.010 (2)
C4	0.077 (3)	0.041 (2)	0.060 (3)	−0.004 (2)	0.004 (2)	0.013 (2)
C3	0.076 (3)	0.048 (3)	0.055 (3)	0.025 (2)	−0.003 (2)	0.017 (2)
C8	0.064 (3)	0.061 (3)	0.049 (3)	0.027 (3)	−0.006 (2)	0.005 (2)
C2	0.051 (3)	0.063 (3)	0.056 (3)	0.010 (2)	−0.016 (2)	0.006 (2)
C7	0.045 (3)	0.066 (3)	0.066 (3)	0.006 (2)	−0.012 (2)	0.000 (2)

Geometric parameters (Å, º)

Cu1—Cl1^{i}	2.7025 (10)	C10—C9	1.370 (5)
Cu1—Cl1	2.3009 (10)	C5—H5	0.9300
Cu1—O1	2.021 (2)	C5—C4	1.380 (6)
Cu1—N1	1.998 (3)	C6—H6	0.9300
Cu1—N2	2.000 (3)	C6—C7	1.372 (5)
O1—N3	1.295 (4)	C9—H9	0.9300
O2—N3	1.242 (4)	C9—C8	1.366 (6)
N1—C1	1.329 (4)	C4—H4	0.9300
N1—C5	1.341 (4)	C4—C3	1.368 (6)
N2—C10	1.332 (5)	C3—H3	0.9300
N2—C6	1.335 (5)	C3—C2	1.375 (6)
O3—N3	1.228 (4)	C8—H8	0.9300
C1—H1	0.9300	C8—C7	1.371 (6)
C1—C2	1.361 (5)	C2—H2	0.9300
C10—H10	0.9300	C7—H7	0.9300
Cl1—Cu1—Cl1^{i}	91.74 (3)	C9—C10—H10	118.8
O1—Cu1—Cl1^{i}	86.11 (8)	N1—C5—H5	118.9
O1—Cu1—Cl1	177.77 (8)	N1—C5—C4	122.1 (4)
N1—Cu1—Cl1	91.59 (9)	C4—C5—H5	118.9
N1—Cu1—Cl1^{i}	94.77 (9)	N2—C6—H6	119.0
N1—Cu1—O1	89.17 (11)	N2—C6—C7	122.0 (4)
N1—Cu1—N2	167.24 (13)	C7—C6—H6	119.0
N2—Cu1—Cl1	90.34 (9)	C10—C9—H9	120.4
N2—Cu1—Cl1^{i}	97.79 (10)	C8—C9—C10	119.2 (4)
N2—Cu1—O1	89.38 (11)	C8—C9—H9	120.4
Cu1—Cl1—Cu1^{i}	88.26 (3)	C5—C4—H4	120.6
N3—O1—Cu1	107.5 (2)	C3—C4—C5	118.9 (4)
C1—N1—Cu1	121.9 (2)	C3—C4—H4	120.6
C1—N1—C5	118.1 (3)	C4—C3—H3	120.6
C5—N1—Cu1	120.0 (2)	C4—C3—C2	118.8 (4)
C10—N2—Cu1	122.7 (3)	C2—C3—H3	120.6
C10—N2—C6	118.2 (3)	C9—C8—H8	120.7
C6—N2—Cu1	119.1 (3)	C9—C8—C7	118.7 (4)

O2—N3—O1	118.0 (3)	C7—C8—H8	120.7
O3—N3—O1	118.4 (3)	C1—C2—C3	119.3 (4)
O3—N3—O2	123.6 (4)	C1—C2—H2	120.4
N1—C1—H1	118.6	C3—C2—H2	120.4
N1—C1—C2	122.8 (4)	C6—C7—H7	120.3
C2—C1—H1	118.6	C8—C7—C6	119.4 (4)
N2—C10—H10	118.8	C8—C7—H7	120.3
N2—C10—C9	122.5 (4)		

Cu1—O1—N3—O2	5.0 (4)	N2—C6—C7—C8	0.4 (7)
Cu1—O1—N3—O3	−175.2 (2)	C1—N1—C5—C4	−0.4 (6)
Cu1—N1—C1—C2	178.8 (3)	C10—N2—C6—C7	1.1 (6)
Cu1—N1—C5—C4	−178.1 (3)	C10—C9—C8—C7	0.9 (7)
Cu1—N2—C10—C9	178.0 (3)	C5—N1—C1—C2	1.2 (6)
Cu1—N2—C6—C7	−178.5 (3)	C5—C4—C3—C2	1.1 (7)
N1—C1—C2—C3	−0.8 (7)	C6—N2—C10—C9	−1.5 (6)
N1—C5—C4—C3	−0.7 (7)	C9—C8—C7—C6	−1.4 (7)
N2—C10—C9—C8	0.5 (6)	C4—C3—C2—C1	−0.4 (7)

Symmetry code: (i) −*x*+1, −*y*+1, −*z*+1.

Hydrogen-bond geometry (Å, º)

D—H···*A*	*D*—H	H···*A*	*D*···*A*	*D*—H···*A*
C4—H4···O1^{ii}	0.93	2.49	3.390 (5)	163
C5—H5···O2^{iii}	0.93	2.57	3.237 (4)	129
C2—H2···Cl1^{iv}	0.93	2.84	3.639 (4)	135

Symmetry codes: (ii) *x*, *y*−1, *z*; (iii) −*x*+1/2, *y*−1/2, −*z*+3/2; (iv) *x*, *y*+1, *z*.